

Supplementary information

Investigation of phase transition, mechanical behavior and lattice thermal conductivity on halogen perovskite using machine learning interatomic potentials

Yong-Bo Shi,<sup>1</sup> Yuanyuan Chen,<sup>1</sup> Haikuan Dong,<sup>1,\*</sup> Hao Wang,<sup>2</sup> and Ping Qian<sup>3,†</sup>

<sup>1</sup>*College of Physical Science and Technology, Bohai University, Jinzhou 121013, PR China*

<sup>2</sup>*Beijing Advanced Innovation Center for Materials Genome Engineering,*

*University of Science and Technology Beijing, Beijing 100083, PR China*

<sup>3</sup>*Department of Physics, University of Science and Technology Beijing, Beijing 100083, PR China*

---

\* [donghaikuan@163.com](mailto:donghaikuan@163.com)  
† [qianping@ustb.edu.cn](mailto:qianping@ustb.edu.cn)

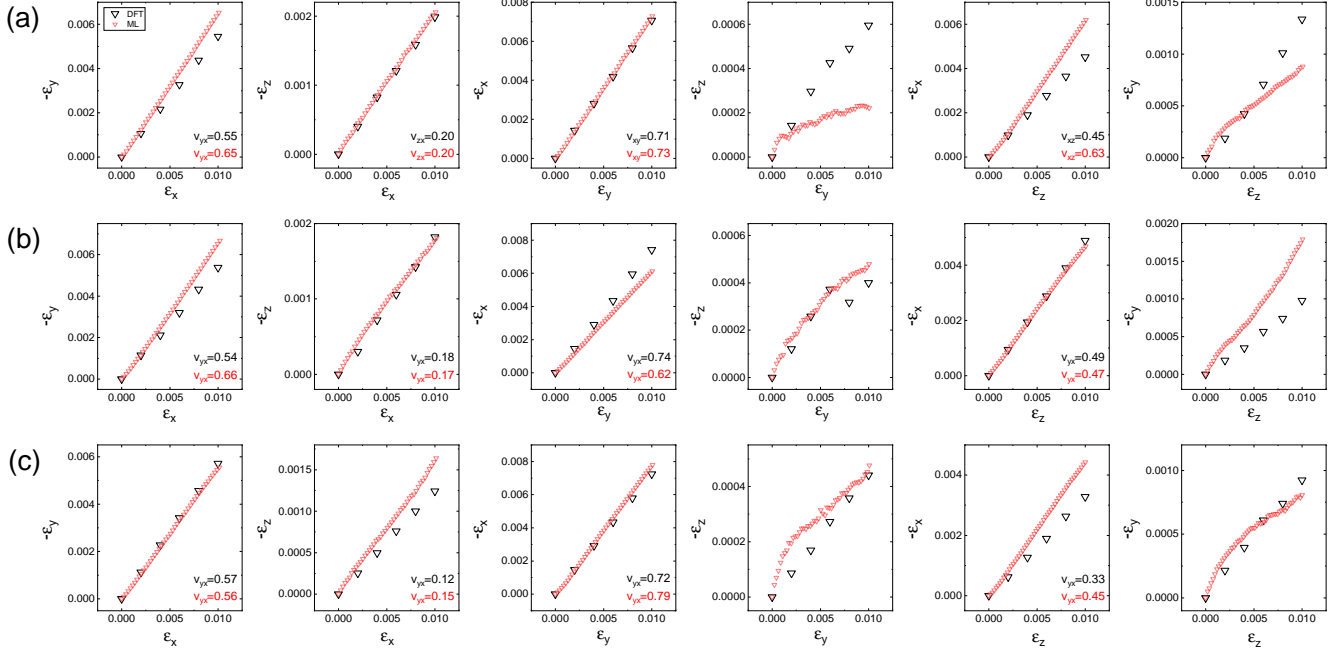


Figure S1. The correlations between the transverse strains (longitudinal coordinates) and applied uniaxial strains (horizontal coordinates) for CsPbX<sub>3</sub> (X=Cl, Br and I), (a) CsPbCl<sub>3</sub>, (b) CsPbBr<sub>3</sub>, (c) CsPbI<sub>3</sub>. The black symbol gives the DFT result. The red symbol represents the NEP-based MD prediction with NpT ensemble at 0.1 K. Poisson's ratio is derived from the slope of the linear fitting, as shown in figure.

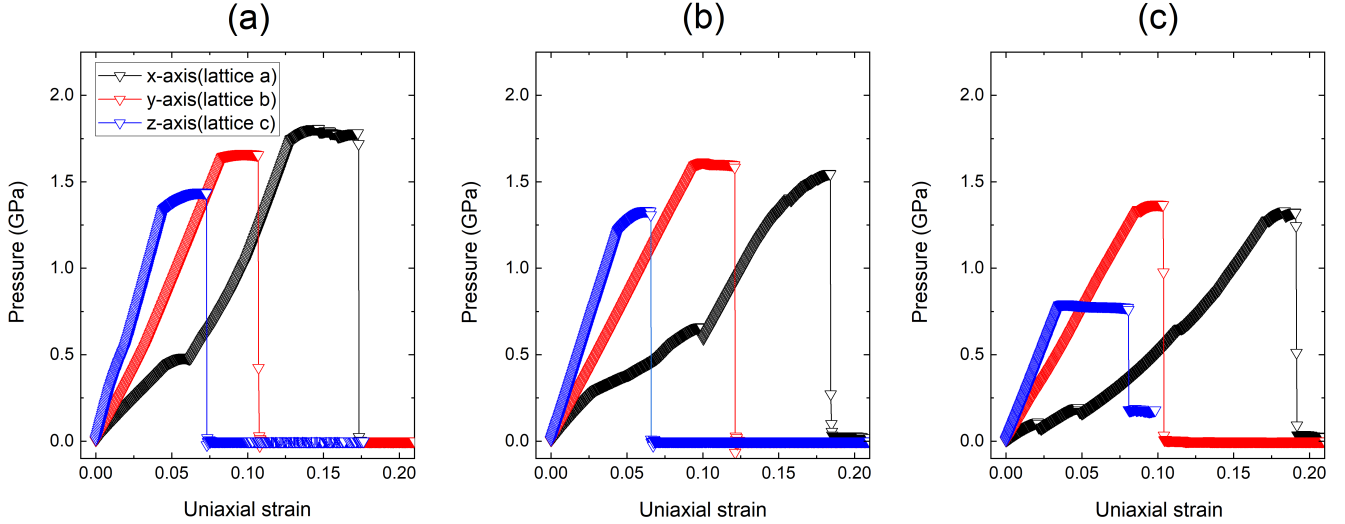


Figure S2. Pressure as a function of uniaxial strain for  $\text{CsPbX}_3$  ( $X=\text{Cl}, \text{Br}$  and  $\text{I}$ ), (a)  $\text{CsPbCl}_3$ , (b)  $\text{CsPbBr}_3$ , (c)  $\text{CsPbI}_3$ . The NEP-based MD simulations with NpT ensemble are performed in a large supercell containing 16000 atoms. The system at 0.10 K is first relaxed for 1 ns to obtain an equilibrium state, and then uniaxial strain is applied to the system with the deformation rate of  $10^{-6} \text{ \AA}/\text{step}$ .

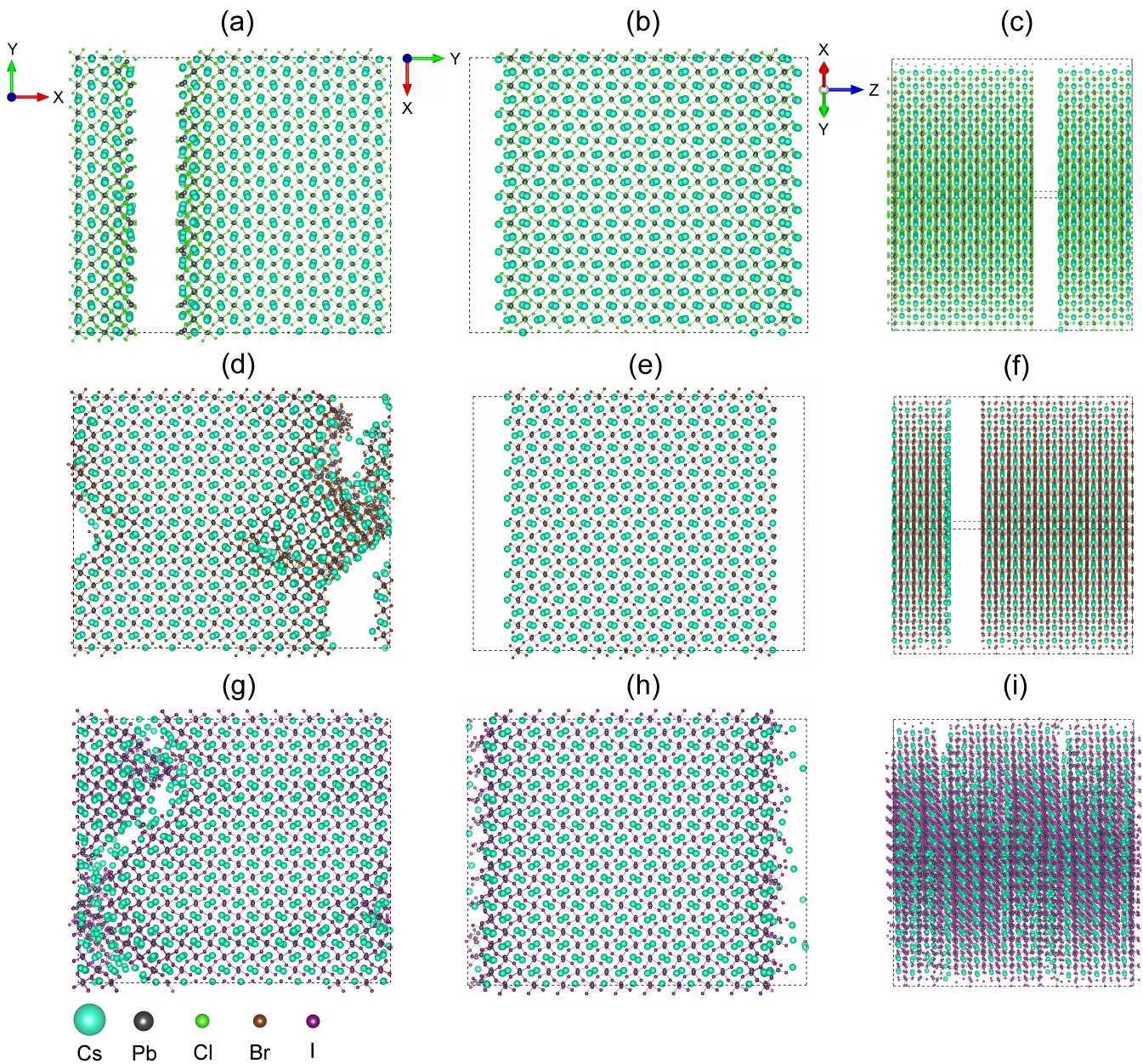


Figure S3. Fracture behavior of the  $\text{CsPbX}_3$  predicted by NEP-based MD simulations with NpT ensemble. (a)-(c) for  $\text{CsPbCl}_3$ , (d)-(f) for  $\text{CsPbBr}_3$ , (g)-(i) for  $\text{CsPbI}_3$ . (a)/(d)/(g), (b)/(e)/(h) and (c)/(f)/(i) represent the strain applied to the  $x$ ,  $y$  and  $z$ -axis, respectively.

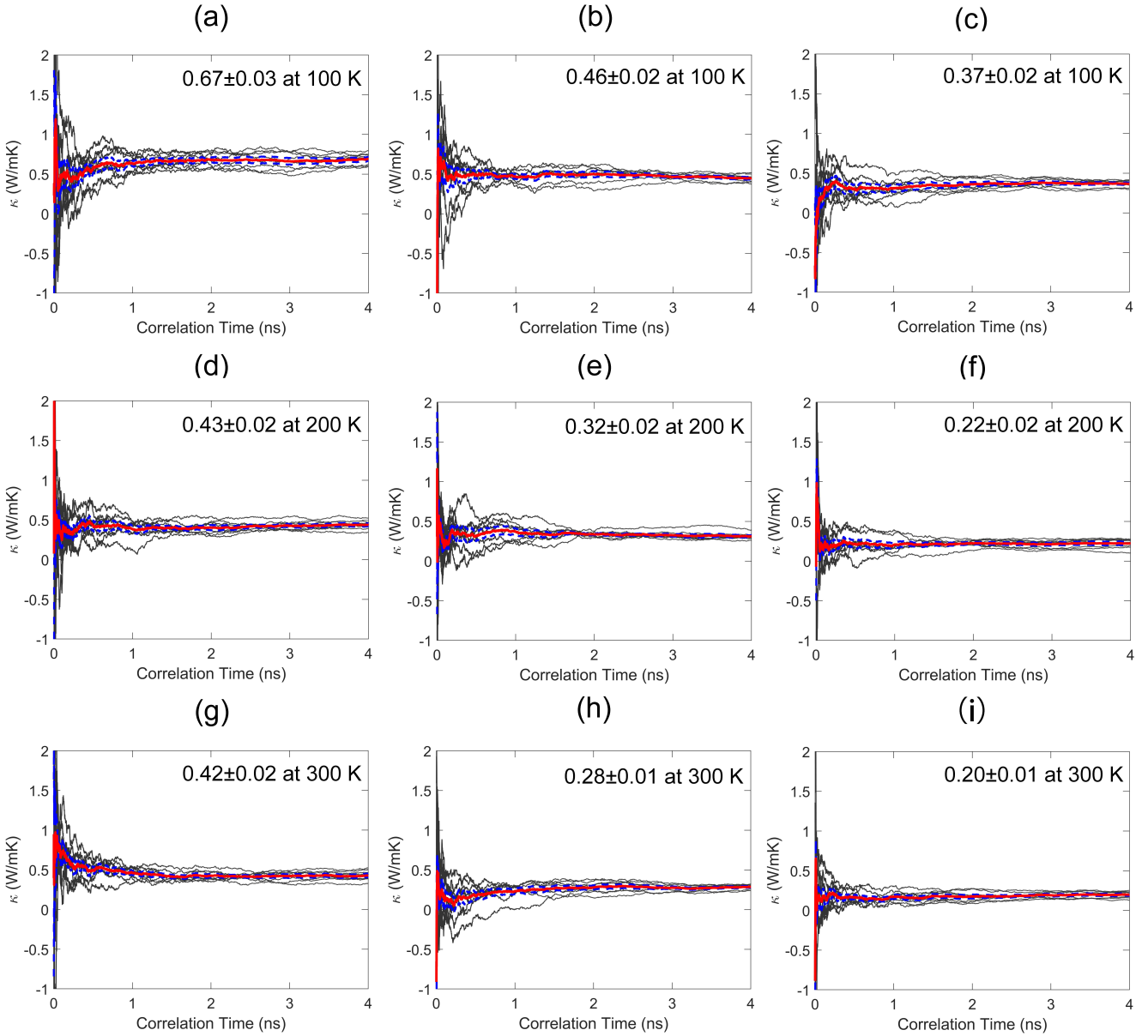


Figure S4. Lattice thermal conductivity of halogen perovskite along  $x$ -axis direction. The black, red solid and blue dashed lines represent 8 independent running, their average value and error bounds, respectively. (a)/(d)/(g), (b)/(e)/(h) and (c)/(f)/(i) represent the results of  $\text{CsPbCl}_3$ ,  $\text{CsPbBr}_3$ ,  $\text{CsPbI}_3$ , respectively.

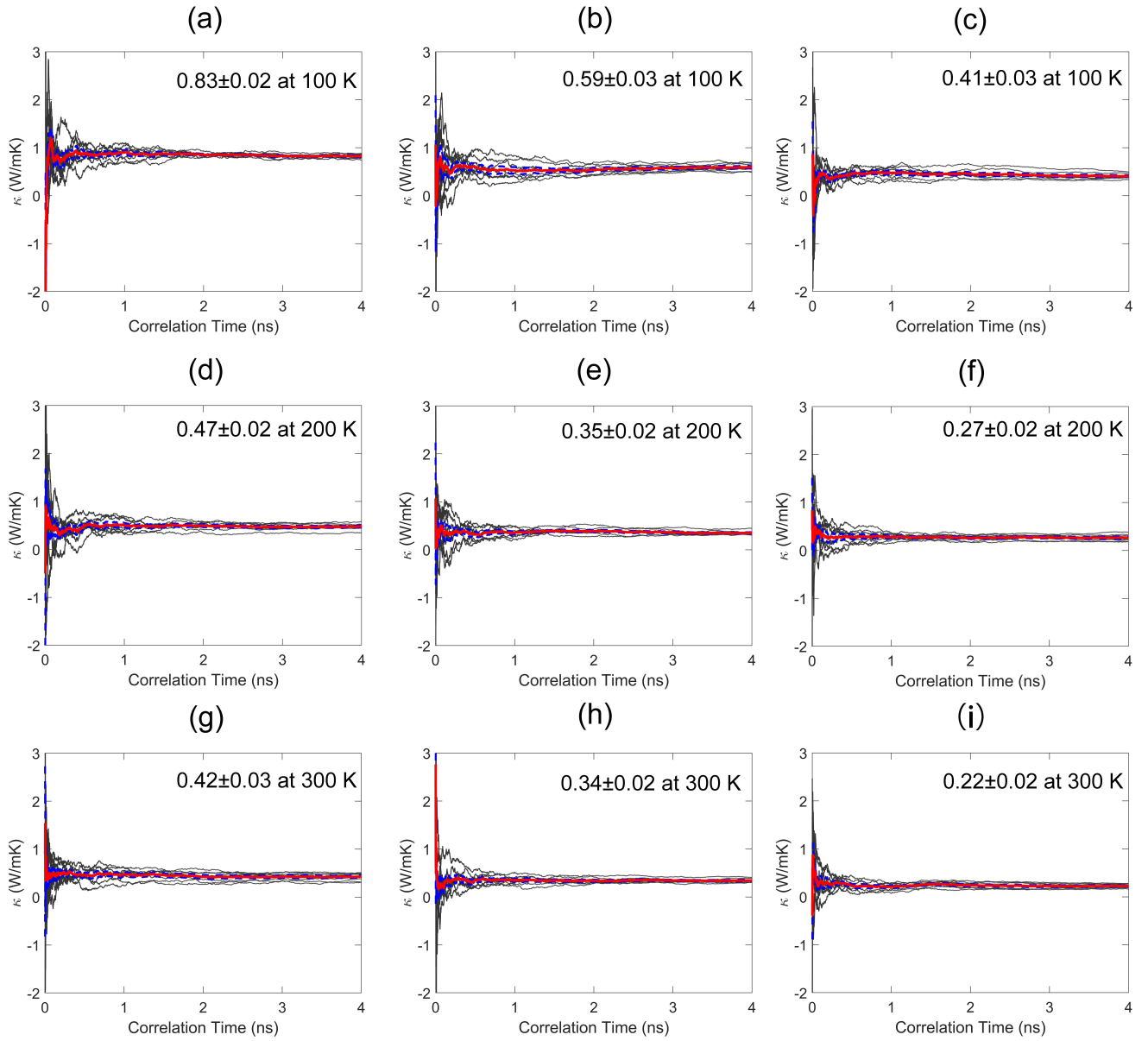


Figure S5. Lattice thermal conductivity of halogen perovskite along  $z$ -axis direction. The black, red solid and blue dashed lines represent 8 independent running, their average value and error bounds, respectively. (a)/(d)/(g), (b)/(e)/(h) and (c)/(f)/(i) represent the results of  $\text{CsPbCl}_3$ ,  $\text{CsPbBr}_3$ ,  $\text{CsPbI}_3$ , respectively.

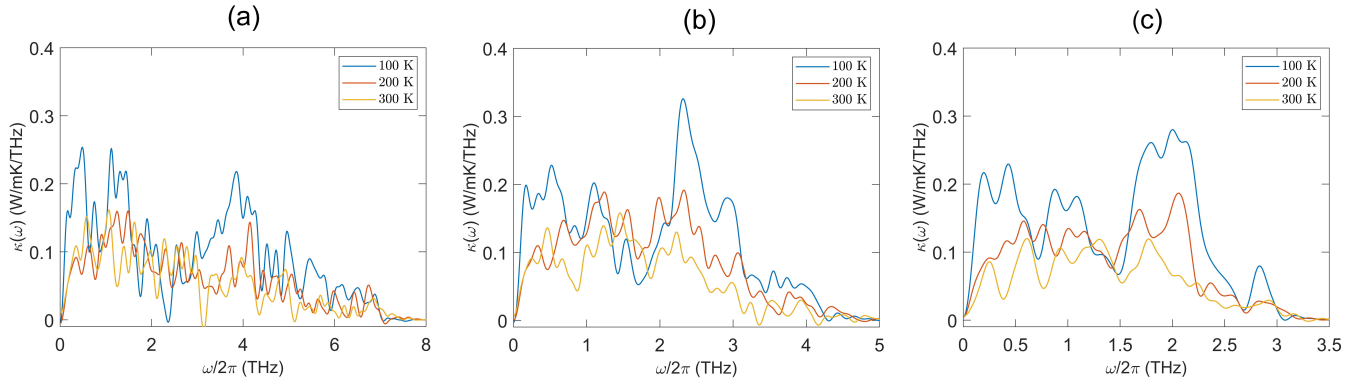


Figure S6. The spectral thermal conductivity of halogen perovskite. (a), (b) and (c) represent the results of  $\text{CsPbCl}_3$ ,  $\text{CsPbBr}_3$ ,  $\text{CsPbI}_3$ , respectively.